Available online at www.sciencedirect.com
ScienceDirect
Analytical Biochemistry 356 (2006) 182–193
ANALYTICAL BIOCHEMISTRY
www.elsevier.com/locate/yabio

Error propagation in relative real-time reverse transcription polymerase chain reaction quantification models: The balance between accuracy and precision

Oddmund Nordgård [a,*], Jan Terje Kvaløy [b,c], Ragne Kristin Farmen [a,1], Reino Heikkilä [a]

[a] Department of Hematology and Oncology, Stavanger University Hospital, 4068 Stavanger, Norway
[b] Department of Mathematics and Natural Science, University of Stavanger, 4036 Stavanger, Norway
[c] Division of Research and Human Resources, Stavanger University Hospital, 4068 Stavanger, Norway

Received 15 March 2006
Available online 14 July 2006

Abstract

Real-time reverse transcription polymerase chain reaction (RT-PCR) has gained wide popularity as a sensitive and reliable technique for mRNA quantification. The development of new mathematical models for such quantifications has generally paid little attention to the aspect of error propagation. In this study we evaluate, both theoretically and experimentally, several recent models for relative real-time RT-PCR quantification of mRNA with respect to random error accumulation. We present error propagation expressions for the most common quantification models and discuss the influence of the various components on the total random error. Normalization against a calibrator sample to improve comparability between different runs is shown to increase the overall random error in our system. On the other hand, normalization against multiple reference genes, introduced to improve accuracy, does not increase error propagation compared to normalization against a single reference gene. Finally, we present evidence that sample-specific amplification efficiencies determined from individual amplification curves primarily increase the random error of real-time RT-PCR quantifications and should be avoided. Our data emphasize that the gain of accuracy associated with new quantification models should be validated against the corresponding loss of precision.
Published by Elsevier Inc.

Keywords: Real-time PCR; RT-PCR; Error propagation; Amplification efficiency

Real-time reverse transcription polymerase chain reaction (RT-PCR)[2] is one of the most sensitive and reliable techniques for mRNA quantification and has achieved widespread application in gene expression analysis during the past few years (reviewed in [1–4]). The technique has two main steps: cDNA synthesis by reverse transcription of mRNA and subsequent quantification of specific cDNAs by real-time PCR. Real-time PCR is based on the real-time monitoring of product formation during the PCR, allowing quantification in the exponential part of the amplification. Amplicon (PCR product) concentration is measured by fluorescence detection, facilitated by the binding of fluorescent dyes or fluorescently labeled sequence-specific probes to the amplicon. Central to real-time PCR is the threshold cycle, C_t (or crossing point, Cp), which is the number of cycles needed to produce a certain defined threshold fluorescence. The threshold fluorescence may be determined by different computational strategies or set manually but must be identical for all samples to be compared within a run. Due to the rather strict exponential nature of PCR it has been possible to construct mathematical models which relate the C_t value to initial template concentration [5–7]. The amplification efficiency of a PCR, here defined as the relative increase in amplicon concentration per cycle, is an important element in these

* Corresponding author. Fax: +47 51 51 89 45.
E-mail address: nood@ext.sir.no (O. Nordgård).
[1] Present address: Gena AS, 4021 Stavanger, Norway.
[2] *Abbreviation used:* RT-PCR, reverse transcription PCR.

0003-2697/$ - see front matter Published by Elsevier Inc.
doi:10.1016/j.ab.2006.06.020

models. The simplest models assume all amplification efficiencies to be equal to 2, whereas more accurate models use amplicon-specific amplification efficiencies [5,7]. Moreover, several methods to determine amplification efficiencies from individual amplification curves have been proposed [8–18].

There are two main strategies for mRNA quantification by real-time RT-PCR: absolute and relative quantification [4]. Absolute quantification is based on standard curves with known amounts of the target molecule. If, as is usually the case, the quantifications are to be performed on cDNA samples from different reverse transcription reactions, this strategy is vulnerable to differences in RNA quality and reverse transcription efficiency. In contrast, with relative quantification the mRNA concentration of interest is determined relative to one or more reference mRNAs in the same cDNA sample [4,7]. This strategy, however, requires stable expression of the reference genes in the samples that are analyzed. In addition, relative quantification strategies may involve normalization against a calibrator sample to improve comparability between multiple experimental runs.

All kinds of measurements are associated with error. Errors are usually divided into two groups: systematic and random errors [19]. Systematic errors lead to systematic deviation from the "true" values and can usually be traced to specific causes. Random errors are due to inherent variations in all aspects of the quantification process and results in spread of repeated quantifications of the same sample. Systematic error influences the accuracy of a measurement, whereas random error causes reduced precision. When, as in relative RT-PCR quantifications, the differences between samples rather than the absolute levels are considered, random errors will be a larger problem than systematic errors. Random errors in observable quantities are usually estimated by computing the standard deviation, which gives a measure for the spread of repeated measurements of the same quantity. However, very often the quantity of interest is determined indirectly by certain computations based on one or several observables. This is in fact, the case with real-time PCR quantifications. From a simple point of view, quantifications are usually done in replicates and standard deviation for the C_t values may be obtained. However, the quantity of interest is the initial template concentration, which is a function of the C_t value and not the C_t value itself. There are random errors involved in the different elements of this function, implying that error propagation may significantly influence the random error of the final result. We therefore decided to analyze the propagation of random error associated with both simple and more advanced mathematical models for relative real-time RT-PCR quantification of mRNA. Theoretical analyses of the different models were tested experimentally. The experimental analyses were performed with clinical RNA samples that had been collected to validate a relative real-time RT-PCR assay to detect minimal residual disease in lymph nodes from operated colorectal cancer patients. The effects on the overall random error from introducing calibrator normalization, multiple reference genes, and sample-specific amplification efficiencies are presented.

Materials and methods

RNA samples

The RNA sample used in the repeated mRNA quantifications was produced by pooling 10 ng total RNA from each of five colon tumors with 5 μg total RNA from each of 10 normal lymph nodes (50.05 μg in total). The normal lymph nodes originated from the resection specimens removed from patients treated for benign colon diseases. The calibrator sample was made by pooling 1 μg total RNA from each of five colon tumors with 5 μg total RNA from each of 9 normal lymph nodes in a similar way. RNA from clinical samples were chosen to validate an assay for minimal residual disease in lymph nodes from colorectal cancer patients. The collecting of clinical samples was approved by the regional ethical committee.

DNase treatment and reverse transcription

Total RNA (50 μg) was treated by 50 U RQ1 DNase (Promega) in a total volume of 500 μl 1× First Strand Synthesis buffer (Invitrogen) containing 500 U RNaseOUT RNase inhibitor. The reaction mixture was incubated at 37 °C for 30 min and inactivated by adding 10 μl RQ1 stop solution and incubating 10 min at 65 °C. Complementary DNA was synthesized by M-MLV reverse transcriptase according to the protocol of the manufacturer (Invitrogen). In detail, 100 μl DNase-treated total RNA (containing 10 μg total RNA) was reverse transcribed in a total volume of 200 μl, containing 10 pg/μl random nonamer, 0.5 mM dNTP, 10 μM dithiothreitol, 2 U/μl RNaseOUT RNase inhibitor, 10 U/μl M-MLV reverse transcriptase, and 20 μl 5× FSS buffer (giving a final concentration of 1× together with the DNase-treated RNA). The reactions were subsequently diluted with water to 1000 μl to obtain a final concentration of 10 ng/μl reverse-transcribed RNA.

Primers

The PCR primers were designed to span exon/exon boundaries. The sequences were CK20-F: 5′-ACCTCC CAGAGCCTTGAGAT-3′, CK20-R: 5′-TGGCTAAC TGGCTGCTGTAA-3′, MUC2-F: 5′-ACTCCAACATCT CCGTGTCC-3′, MUC2-R: 5′-AGCCACACTTGTCTG CAGTG-3′, BCR-F: 5′-GCTCTATGGGTTTCTGAAT G-3′, BCR-R: 5′-AAATACCCAAAGGAATCCAC-3′, HPR-T1-F: 5′-TTCCTTGGTCAGGCAGTA-3′, and HPRT1-R: 5′-TATCCAACACTTCGTGGG-3′. The amplicon sizes were 106, 111, 99, and 81 bp for CK20, MUC2, BCR, and HPRT1, respectively.

Real-time PCR set up

PCR amplifications were performed with the qPCR SYBR Green Core kit from Eurogentec according to the manufacturer's recommendations. Twenty nanograms of reverse transcribed RNA was amplified in a total volume of 25 µl 1× reaction buffer containing 0.2 mM dNTP, 0.15 µM primers, 0.75 µl 1:200 diluted SYBR Green in dimethyl sulfoxide, and 2.5, 1.5, 2, and 2 mM $MgCl_2$ for the CK20, MUC2, BCR, and HPRT1 reactions, respectively. All components except the template were added to 96-well PCR plates as mastermixes. The amplifications were performed in an Mx3000P (Stratagene) real-time PCR instrument, incubating 10 min at 94 °C and then 40 cycles of 20 s at 94 °C and 30 s at 60 °C. Subsequently, the reaction products were analyzed by melting curves. All melting curves revealed well-defined peaks with the expected melting temperatures, confirming the specificity of the primers at the reaction conditions. Amplicon identities were also confirmed by sequencing. Mean cycle threshold values were 28.58, 28.29, 20.66, and 22.57 in the unknown sample and 21.68, 19.62, 20.63, and 22.47 in the calibrator sample for the CK20, MUC2, BCR, and HPRT1 amplifications, respectively. Amplification curves and dissociation curves from a randomly selected experiment are available as supplemental material on the journal website (S1). A three-point smoothing algorithm was applied to all amplification curves except those used for determination of amplification efficiencies for individual amplification curves. Reaction setup, template addition, and thermocycling were performed in three separate areas of the lab. No-template controls were included in every run to monitor potential contamination.

Amplicon-specific amplification efficiencies were determined by the standard curve method performed on four different samples in three replicated experiments. Each of the target gene standard curves consisted of a six-point fourfold dilution series analyzed in duplicates, whereas the reference gene standard curves consisted of five-point fourfold dilution series analyzed in duplicates (mean R^2 for all 48 standard curves was 0.996). Mean amplification efficiencies for the CK20, MUC2, BCR, and HPRT1 amplicons were 1.96 ± 0.03, 1.99 ± 0.02, 2.03 ± 0.03, and 2.03 ± 0.03, respectively.

Mathematical models for relative real-time RT-PCR quantification

The exponential phase of a PCR can be described by the following equation:

$$T = T_0 \cdot E_T^C, \tag{1}$$

where T is the number of target molecules after C cycles of PCR, T_0 is the initial number of target molecules, and E_T is the amplification efficiency of the target amplicon. The fluorescent DNA-binding dye or probe that is added to the reactions allows PCR product concentration to be measured by fluorescence detection. The threshold cycle, C_t (or crossing point, Cp, in LightCycler terminology), is the number of cycles needed to produce a certain defined threshold fluorescence. The number of target molecules producing the threshold fluorescence (T_{C_t}) is then given by

$$T_{C_t} = T_0 \cdot E_T^{C_t}. \tag{2}$$

Relative quantification in its simplest form expresses the relative amount of target mRNA as the ratio r_1 between the initial number of target molecules, T_0, and the initial number of reference mRNA molecules, denoted R_0 below. From Eq. (2) it can be shown that [5,10]

$$r_1 = \frac{T_0}{R_0} = \frac{T_{C_{t,T}} \cdot E_T^{-C_{t,T}}}{R_{C_{t,R}} \cdot E_R^{-C_{t,R}}}. \tag{3}$$

In the same experiment $T_{C_{t,T}}$ and $R_{C_{t,R}}$ are constants. Thus,

$$r_1 = \frac{T_0}{R_0} = k \cdot \frac{E_T^{-C_{t,T}}}{E_R^{-C_{t,R}}}, \tag{4}$$

where k is a constant that is not necessarily equal to 1. The value of k depends on several factors, such as the type of chemistry used, the sizes of the PCR products, the sequence of the PCR products, and the setting of the fluorescence threshold [5]. Thus, it is not strictly correct to assume that k is constant in multiple runs of the same assay. The constant k can be eliminated by normalization against a calibrator sample. The calibrator could be a reference sample that is included in all runs, an untreated control, or a randomly chosen sample, depending on the experimental setup. The relative expression level r_2 of the target gene in the sample relative to the calibrator sample is then given by [5,7]

$$r_2 = \frac{\frac{T_0}{R_0}}{\frac{T_{0,\mathrm{cal}}}{R_{0,\mathrm{cal}}}} = \frac{k \cdot \frac{E_T^{-C_{t,T}}}{E_R^{-C_{t,R}}}}{k \cdot \frac{E_T^{-C_{t,T,\mathrm{cal}}}}{E_R^{-C_{t,R,\mathrm{cal}}}}} \quad \text{and} \tag{5}$$

$$r_2 = \frac{E_T^{C_{t,T,\mathrm{cal}} - C_{t,T}}}{E_R^{C_{t,R,\mathrm{cal}} - C_{t,R}}}. \tag{6}$$

Livak and Schmittgen [5] simplified this expression by assuming that the amplification efficiencies of both amplicons were equal to 2, an assumption that has to be validated. This gives the following expression (the $2^{\Delta\Delta C_t}$ method [5])

$$r_3 = 2^{\Delta\Delta C_t}, \tag{7}$$

where $\Delta\Delta C_t = C_{t,T,\mathrm{cal}} - C_{t,T} + C_{t,R} - C_{t,R,\mathrm{cal}}$. The amplification efficiency was expressed as $E \approx 2$ instead of $E - 1 \approx 1$ in the present paper to simplify the expressions (as in [7,13]).

Error propagation

If the quantity of interest y is a function of n observables $x_1, x_2, \ldots, x_n$, it can be shown that the standard deviation of y is approximated by

$$\mathrm{sd}(y) = \sqrt{\sum_{k=1}^{n}\left(\left(\frac{\delta y}{\delta x_k}\right)^2 \cdot \mathrm{var}(x_k)\right) + \sum_{i=2}^{n}\sum_{j=1}^{i-1}\left(2 \cdot \frac{\delta y}{\delta x_i} \cdot \frac{\delta y}{\delta x_j} \cdot \mathrm{cov}(x_i, x_j)\right)}, \tag{8}$$

where $\mathrm{var}(x_k)$ is the variance of the observable x_k, $\mathrm{cov}(x_i, x_j)$ is the covariance between x_i and x_j, and $\frac{\delta y}{\delta x_k}$ is the partial derivative of y with regard to x_k [19,20]. If the observables are uncorrelated, the covariance terms can be omitted [19]. Eq. (8) is also known as the error propagation formula. We used this equation to calculate error propagation expressions for the various mathematical models of relative real-time RT-PCR quantification.

Computations

Cycle threshold values and raw fluorescence data were exported from the Mx3000P software (Stratagene) via Microsoft Excel to simple text files and imported into the R software package (http://www.r-project.org). All subsequent computations except the LinRegPCR regressions were performed with the R software package. The R functions implementing the Tichopad and Liu/Saint algorithms are available as supplemental material on the journal website (S2 and S3).

The intrarun variation in amplification efficiency was compared with the interrun variation by one-way analysis of variance (ANOVA). The distributions of the amplification efficiencies were judged to be near normal by visual inspection of QQ plots.

Results

Estimation of propagated error in real-time PCR

The random error observed in real-time reverse transcription PCR originates from both the reverse transcription step and the PCR amplification step [21]. We wanted to analyze the propagation of error associated with the various mathematical models of relative real-time PCR quantification and therefore focused on the PCR step. Assuming that the amplification efficiencies of both the target amplicon and the reference amplicon are equal to 2 in Eq. (4) (Materials and methods), we obtained the simplest expression for relative RT-PCR quantification (here denoted the $2^{\Delta C_t}$ method),

$$r_4 = \frac{T_0}{R_0} = k \cdot 2^{\left(C_{t,R} - C_{t,T}\right)}, \tag{9}$$

where k is a constant, T_0 is the initial amount of target transcript, R_0 is the initial amount of reference transcript, and $C_{t,R}$ and $C_{t,T}$ are the C_t values corresponding to the reference and target transcript amplifications, respectively. We applied the error propagation formula (Eq. (8)) to obtain an expression for the propagated error associated with r_4:

$$\mathrm{sd}(r_4) = \sqrt{\left(\frac{\delta r_4}{\delta C_{t,R}}\right)^2 \mathrm{var}(C_{t,R}) + \left(\frac{\delta r_4}{\delta C_{t,T}}\right)^2 \mathrm{var}(C_{t,T}) + 2\left(\frac{\delta r_4}{\delta C_{t,R}}\right)\left(\frac{\delta r_4}{\delta C_{t,T}}\right)\mathrm{cov}(C_{t,T}, C_{t,R})}, \tag{10}$$

$$\mathrm{sd}(r_4) = \sqrt{(ln2 \cdot r_4)^2 \mathrm{var}(C_{t,R}) + (-ln2 \cdot r_4)^2 \mathrm{var}(C_{t,T}) + 2(ln2 \cdot r_4)(-ln2 \cdot r_4)\mathrm{cov}(C_{t,T}, C_{t,R})}, \tag{11}$$

$$\frac{\mathrm{sd}(r_4)}{r_4} = ln2\sqrt{\mathrm{var}(C_{t,T}) + \mathrm{var}(C_{t,R}) - 2\mathrm{cov}(C_{t,T}, C_{t,R})}. \tag{12}$$

Thus, the relative standard deviation (coefficient of variation) of the relative expression level given by Eq. (9) can be directly estimated from the variances and covariances of the C_t values. From this expression it is evident that reference genes with high reproducibility are preferable with regard to the overall precision of the quantitation.

Although quantification experiments may be performed as single-run assays, multirun quantifications are required in most clinical studies. The error propagation expression in Eq. (12) can be applied to both intra- and interrun error analyses. When considering intraassay variation in singleplex assays (quantitating only one transcript per reaction), there is obviously no correlation between the C_t values of the target and the reference genes and the covariance term can be omitted. When employing multiplex assays (quantitating both target and reference transcripts in the same reaction) or when considering any interassay variation, however, the covariance has to be checked. Thus, we quantitated two target mRNAs and two reference mRNAs in duplicates from the same cDNA sample in 10 successive runs with a singleplex real-time PCR assay. To minimize the correlation of the C_t values, the same fluorescence threshold was used in all runs. Plotting the C_t values for the different mRNAs against each other and computing the covariances showed that the C_t values of the different transcripts were all correlated across the runs (Fig. 1 and Table 1). The covariances were of similar magnitude as the variances, implying that covariance had to be accounted for in interassay error estimates. However, Eq. (12) shows that the covariance term actually has a negative sign and thus a positive covariance does not increase the overall random error of the quantification. We compared error propagation estimates obtained by Eq. (12) with the coefficient of variation (CV) of r_4 (Eq. (9)) computed for each of the 10 experiments described above and found good agreement (Table 2).

Calibrator normalization and error propagation

To use the expression in Eq. (9) for multirun quantifications, one must assume that k is constant throughout the runs, an assumption that has to be validated. To eliminate this constant, normalization against a cal-

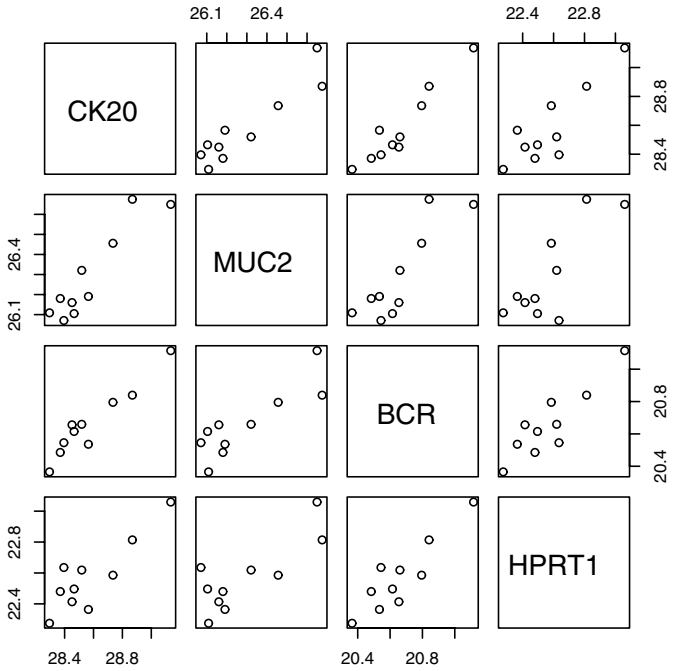

Fig. 1. Correlation plot showing C_t values for the CK20, MUC2, BCR, and HPRT1 transcripts determined in duplicates of the same sample in ten repeated experiments. Each subplot shows the C_t values of two transcripts plotted against each other. The C_t values of CK20, MUC2, BCR, and HPRT1 are plotted on the x axis of the plots in the first, second, third, and fourth columns of subplots, respectively, as indicated on the diagonal. Similarly, the C_t values of CK20, MUC2, BCR, and HPRT1 are plotted on the y axis of the plots in the first, second, third, and fourth rows of subplots, respectively. Each point represents the mean of the two duplicates quantitated in a single run.

Table 1
Covariances of the C_t values for different transcripts

Transcript	CK20	MUC2	BCR	HPRT1
CK20	0.068[a]	0.054	0.053	0.052
MUC2	0.054	0.051[a]	0.042	0.042
BCR	0.053	0.042	0.045[a]	0.044
HPRT1	0.052	0.042	0.044	0.053[a]

[a] Variance.

Table 2
Coefficients of variation (%) for the quantification of CK20 and MUC2 mRNA

Reference[a]	CK20		MUC2	
	Computational[b]	Experimental	Computational[b]	Experimental
BCR	5.9	5.9	7.9	7.8
HPRT1	9.0	9.2	9.8	10.1

[a] Target mRNA concentrations were normalized against reference mRNA concentrations.
[b] Estimated by the error propagation formula.

ibrator sample has been introduced as given in Eqs. (6) and (7) (Materials and methods). From Eq. (8) it can be shown that the relative standard deviation (=CV) of r_3 in Eq. (7) (the $2^{\Delta\Delta C_t}$ method) can be estimated by

$$\frac{\mathrm{sd}(r_3)}{r_3} = ln2\sqrt{\mathrm{var}(C_{t,T}) + \mathrm{var}(C_{t,T,\mathrm{cal}}) + \mathrm{var}(C_{t,R}) + \mathrm{var}(C_{t,R},\mathrm{cal}) + \mathrm{COV}_1}, \quad (13)$$

where $\mathrm{COV}_1 = -2\mathrm{cov}(C_{t,T},C_{t,T,\mathrm{cal}}) - 2\mathrm{cov}(C_{t,T},C_{t,R}) + 2\mathrm{cov}(C_{t,T},C_{t,R,\mathrm{cal}}) + 2\mathrm{cov}(C_{t,T,\mathrm{cal}},C_{t,R}) - 2\mathrm{cov}(C_{t,T,\mathrm{cal}},C_{t,R,\mathrm{cal}}) - 2\mathrm{cov}(C_{t,R},C_{t,R,\mathrm{cal}})$. From this expression it is evident that the random error of the calibrator C_t values and the random error of the sample C_t values contribute similarly to the overall error. Thus, a calibrator sample with minimal variance should be chosen. This can be achieved by using a sample with high concentrations of the transcripts of interest as calibrator, since the precision of real-time PCR is usually better for higher target concentrations [1,22]. With this theoretical background, we tested in our experimental system the magnitude of the loss of precision resulting from the normalization against a calibrator. This was compared to the potential error introduced by assuming that the constant k in Eq. (9) is constant in multiple runs of the same experiment. Duplicate quantifications of the target transcripts of interest and the two reference transcripts in aliquots of the same sample and a calibrator sample were performed in 10 separate experiments. The variances of the C_t values of the sample and the calibrator were of similar magnitude (results not shown). Error estimation by Eqs. (12) and (13) indicated that the random error in the relative quantifications would be substantially higher with calibrator normalization than without, given a constant k (results not shown). We computed the relative concentration of each transcript of interest against each of the two reference transcripts for the 10 experiments with the $2^{\Delta C_t}$ (Eq. (9)) and $2^{\Delta\Delta C_t}$ methods (Eq. (7)) and deter-

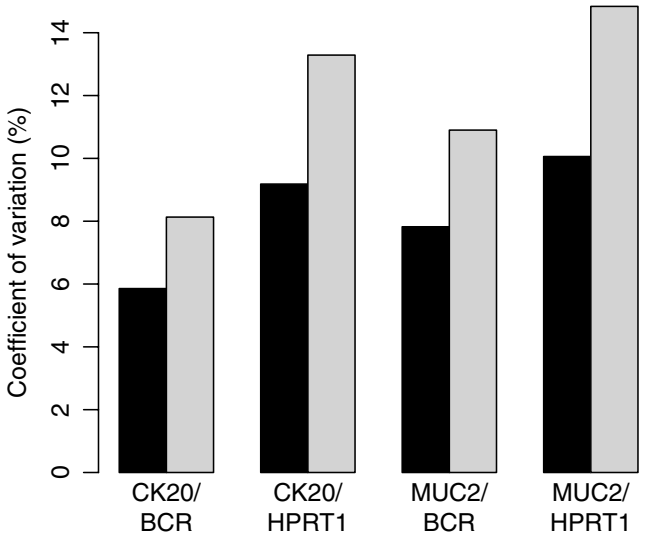

Fig. 2. Coefficients of variation (%) in repeated relative quantifications determined by the $2^{\Delta C_t}$ method (black bars) versus the $2^{\Delta\Delta C_t}$ method (gray bars). The two target mRNA concentrations (CK20 and MUC2) were computed relative to the two reference mRNAs (BCR and HPRT1).

mined the CVs. As can be seen in Fig. 2, the CVs were consistently larger for the $2^{\Delta\Delta C_t}$ method. This indicated that the constant k must have been fairly stable across the runs in this experimental system, eliminating the need for a calibrator. Other experimental systems may perform differently, emphasizing the necessity of validation before omitting the calibrator normalization.

Multiple reference genes and error propagation

There is considerable evidence that no perfect universal reference gene for relative quantification of gene expression exists [23–28]. The expression stability of candidate reference genes must be validated in the relevant experimental system. To minimize the error due to variations in reference gene expression level, normalization against the geometric mean of multiple reference transcript concentrations has been proposed [24]. We augmented the Pfaffl model [7] to include two reference genes according to this proposition and evaluated the corresponding propagation of error. First, the augmented model for relative quantification with two reference transcripts was established,

$$r_4 = \frac{E_T^{C_{t,T,\mathrm{cal}} - C_{t,T}}}{\sqrt{E_{R1}^{C_{t,R1,\mathrm{cal}} - C_{t,R1}} \cdot E_{R2}^{C_{t,R2,\mathrm{cal}} - C_{t,R2}}}}, \tag{14}$$

where $R1$ and $R2$ represented the two reference transcripts, respectively. We then applied Eq. (8) and developed the error propagation expression for this model,

$$\frac{\mathrm{sd}(r_4)}{r_4} = \sqrt{V_T + V_{R1} + V_{R2} + \mathrm{COV}_2}, \tag{15}$$

where $V_T = (\log E_T)^2 \cdot (\mathrm{var}(C_{t,T,\mathrm{cal}}) + \mathrm{var}(C_{t,T}))$, $V_{R1} = (0.5 \cdot \log E_{R1})^2 \cdot (\mathrm{var}(C_{t,R1,\mathrm{cal}}) + \mathrm{var}(C_{t,R1}))$, $V_{R2} = (0.5 \cdot \log E_{R2})^2 \cdot (\mathrm{var}(C_{t,R2,\mathrm{cal}}) + \mathrm{var}(C_{t,R2}))$, and COV_2 represents the covariance terms, which are left unexpanded due to their length. Eq. (15) indicates that the addition of an extra reference gene does not increase the overall random error of the quantification (notice the 0.5^2 terms). If there is no covariance and equal amplification efficiencies and variances for all transcripts are assumed, it can be shown that the estimated CV when normalizing against two reference transcripts is only 87% ($\frac{\sqrt{3}}{2}$) of the CV when normalizing against a single reference transcript. This was confirmed by simulation, selecting random C_t values from the same normal distribution (results not shown). However, in real experiments the covariance complicates the computations. We applied the model in Eq. (14) to our data for the two target amplicons CK20 and MUC2 in the 10 repeated quantifications described above and computed the CV for the relative quantifications with two reference transcripts (Fig. 3). We compared the precision of this quantification with those of the single reference gene cases and concluded that normalization against an additional reference gene did not increase the overall random error. Rather, the CVs of the two-reference gene quantifications were found to be equal to or somewhat lower than the mean of the CVs for each single-reference gene quantification (10.0% versus 10.7% and 12.2% versus 12.8%). Thus, error propagation does not seem to be an argument against multiple reference gene normalization, neither theoretically nor experimentally, in our system. However, it is preferable that the reproducibilities of all the reference genes are good, since the least reproducible reference gene will have considerable impact upon the overall random error. With respect to error propagation, a single very reproducible reference transcript may perform better alone than in combination with a reference transcript assay that has poor reproducibility. The reproducibility of reference transcript quantification can be optimized by choosing reference genes with high expression levels, since the reproducibility of real-time RT-PCR is usually better at higher target concentrations [1,22].

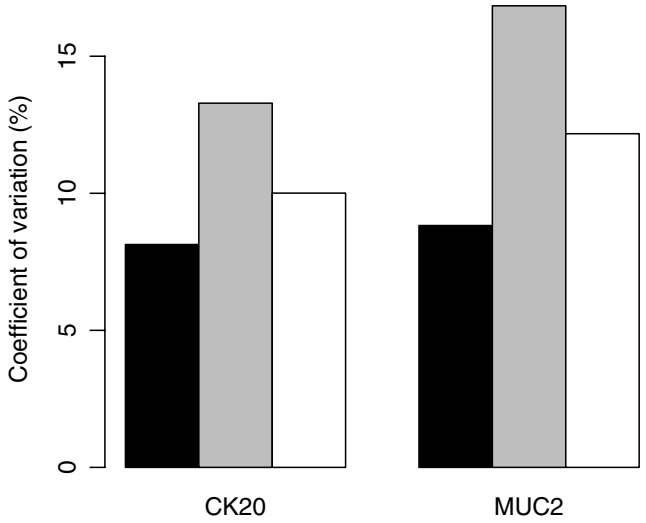

Fig. 3. Coefficient of variation (%) for the relative quantification of CK20 and MUC2 mRNA versus single or multiple reference genes. Black bars show the results for BCR alone as a reference gene, gray bars show the results for HPRT1 alone, and white bars show the results when using the geometric mean of both reference genes as a normalization factor.

Amplification efficiency and error propagation

Amplification efficiencies of specific amplicons have typically been determined by the generation of dilution curves and the plotting of the C_t values against the logarithm of the initial concentration (the standard curve method) [6]. Using specific amplification efficiencies for each amplicon instead of the ideal value 2 obviously results in more correct quantifications [7]. There is, however, evidence that the amplification efficiency of the same amplicon varies from sample to sample, due to small amounts of different PCR inhibitors [15,17,29,30]. To correct for this variation, several methods for the determination of amplification efficiency from individual amplification curves have been developed. Some researchers have reported algorithms that are based on regression of the exponential part of the amplification curve [8,10,12–16]. Other strategies involve

four-parametric sigmoidal fit of the entire amplification curve [9,11,17,18,31].

We determined the amplification efficiencies from individual amplification curves by applying three of the referred algorithms to the 10 quantifications of the same sample already described. In detail, this included the LinRegPCR program made by Ramakers et al. [12], the exponential fit algorithm of Tichopad and co-workers [16] (here denoted the Tichopad method), and the four-parametric sigmoidal fit algorithm of Liu and Saint [9] (Liu/Saint method). Mean amplification efficiencies are shown in Fig. 4. The three methods produced quite different results, indicating that at least two of the methods gave poor estimates of the true amplification efficiency. Consistently, the Tichopad method gave lower amplification efficiency than the LinRegPCR program, whereas the precision seemed to be better for the sigmoidal-fit method of Liu and Saint than for the two other methods. Nevertheless, there was considerable variation in the determined amplification efficiencies of the runs. We asked whether this variation reflected a true variation in amplification efficiency of the reactions or whether it could be due to random error introduced by the method of determination. There was no correlation between the methods (results not shown), suggesting that the efficiency variation did not reflect a true interassay efficiency variation. Considering that the precision of the pipetting of template is very high compared with the total variability of the quantifications (the pipette performance information from the manufacturer states that the precision of the pipette under optimal usage is 0.7% (CV)), we assumed that the addition of template (T_0) in each duplicate was constant. In the same run, the amount of a specific PCR product at fluorescence threshold (T) is also constant. Thus, the following expression should be constant for each duplicate in each run (derived from Eq. (1)):

$$\frac{T}{T_0} = E_T^{Ct}. \tag{16}$$

We computed E_T^{Ct} for each reaction in the 10 duplicates described above with amplification efficiencies determined by the LinRegPCR, Tichopad, and Liu/Saint algorithms. We estimated the random error of the three methods by computing the CV for each duplicate. For comparison, similar computations were done with constant amplification efficiency determined previously by the standard curve method. Mean CVs for the four studied transcripts are shown in Fig. 5. The variability of E_T^{Ct} was much higher when using amplification efficiencies for each reaction instead of a constant previously determined efficiency, indicating that the variations in the individually determined amplification efficiencies represent primarily random error of the determination and not a real variation. The variation in E_T^{Ct} was significantly higher than the expected pipetting variation, confirming the validity of our assumption that T_0 is constant in this system. Moreover, the precision of these quantifications differed substantially for the three methods. We observed an increasing precision in the following order: LinRegPCR, Tichopad and Liu/Saint. We also performed one-way ANOVA to test the null hypothesis that there is no difference in amplification efficiency in the runs. As expected, we were not able to reject the null hypothesis for any of the methods or amplicons ($p > 0.15$).

Having characterized the interassay variation of the reaction-specific amplification efficiencies as primarily random error of the estimations, we proceeded to investigate the consequence of using these amplification efficiencies in the relative quantification models. We determined the

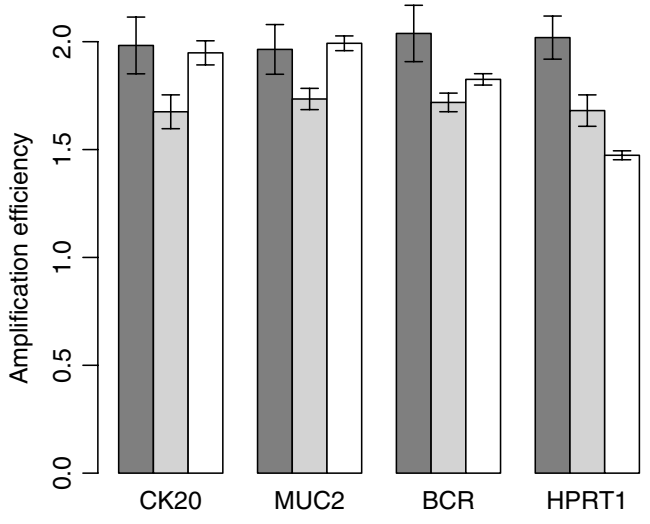

Fig. 4. Mean amplification efficiencies of the CK20, MUC2, BCR, and HPRT1 amplicons in aliquots of the same sample determined from individual amplification curves by the LinRegPCR (dark gray bars), Tichopad (light gray bars), and Liu/Saint (white bars) algorithms. Standard deviations are shown by error bars.

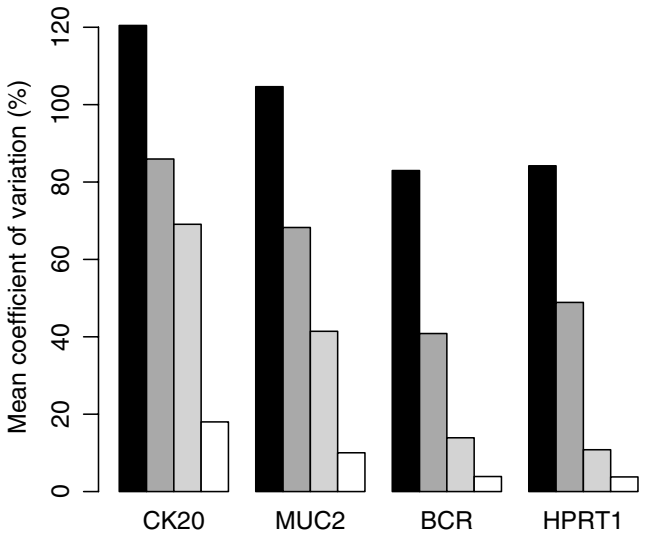

Fig. 5. Variability of E^{C_t} when using amplification efficiencies determined for each reaction by the LinRegPCR (black bars), the Tichopad (dark gray bars), and the Liu/Saint (light gray bars) algorithms or kept constant (white bars). Mean coefficients of variation (%) of E^{C_t} were computed for each of 10 duplicates and averaged.

relative amounts of CK20 and MUC2 versus both BCR and HPRT1 in each of the 10 replicated duplicates of the same sample by the simple expression in Eq. (4) (without calibrator normalization) and by the Pfaffl model in Eq. (6) (with calibrator normalization). The amplification efficiencies were estimated from individual amplification curves using the three algorithms described above and compared with a constant predetermined amplification efficiency. Fig. 6 shows the CV (%) for the two quantification models. The reproducibility was consistently better when using a constant amplification efficiency compared to that when using the sample-specific amplification efficiencies. The extremely high CVs (up to 250%) reflect the exponential nature of the PCR quantification models. Errors in the base number (amplification efficiency) are more severe than errors in the exponent (threshold cycle).

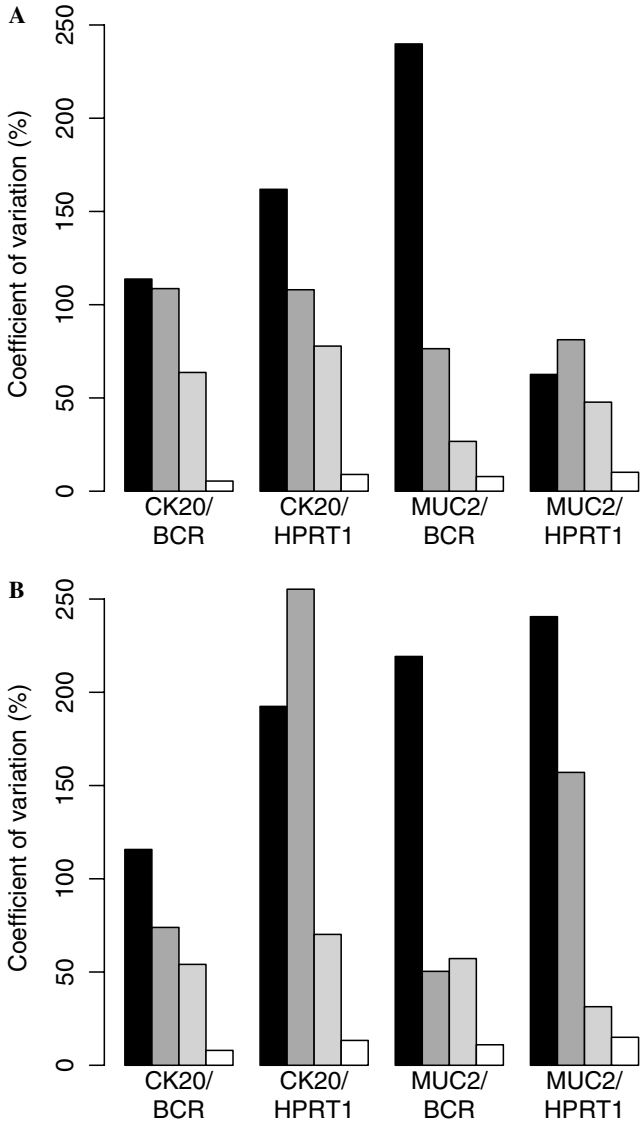

Fig. 6. Coefficients of variation (%) of relative real-time RT-PCR quantification when using amplification efficiencies determined for individual amplification curves. (A) Relative amounts of the target transcripts were determined according to the model in Eq. (4) (without calibrator normalization). (B) Relative amounts of the target transcripts were determined according to the Pfaffl model in Eq. (6) (with calibrator normalization). Amplification efficiencies were determined by the LinRegPCR (black bars), the Tichopad (dark gray bars), and the Liu/Saint (light gray bars) algorithms or kept constant (white bars). Mean amplification efficiencies for each duplicate were used in the computations.

We applied the error propagation formula (Eq. (8)) to the quantification models in Eqs. (4) and (6), treating the amplification efficiencies as observables. The resulting expressions are available at the journal website as supplemental material (S4). Amplification efficiencies are strictly speaking not an observable in this setting but are derived from raw fluorescence data by regression. Thus, their variability may be estimated from the regression parameters as described for linear regression by Marino et al. [13]. However, to avoid unnecessary complexity, we treated amplification efficiencies as observables with variances derived from replicated quantifications of the same sample. The referred error propagation expressions (supplemental material) indicated that the contribution of the amplification efficiency error to the overall random error should be less when applying calibrator normalization. However, for most combinations of target and reference transcripts we did not observe any error reduction when normalizing against a calibrator (Fig. 6A versus Fig. 6B), possibly due to a considerable countereffect from the addition of the new observables associated with the calibrator.

Discussion

Along with the development of instruments and chemistries for real-time PCR, computational models of varying complexity have emerged, generally with the intention to reduce systematic errors. However, the development of new models for relative real-time RT-PCR quantification has generally paid little attention to the aspect of random error and error propagation. We have applied the principles of error propagation to the most established mathematical models for real-time RT-PCR quantification and have evaluated, both theoretically and experimentally, the contribution of various model elements to the overall random error. Calibrator normalization was shown to increase the overall random error of the quantifications in our system, emphasizing that the requirement for a calibrator should be evaluated for each experimental setup. In contrast, we found that normalization against the geometric mean of two reference transcript concentrations compared to a single reference transcript may indeed be preferable, as it did not increase the overall random error of the quantifications. Finally, we explored different approaches to determine sample-specific amplification efficiencies from individual amplification curves and presented evidence that the efficiency variations observed for the same sample represent primarily random error of the efficiency determination. Incorporation of sample-specific amplification efficiencies in the relative quantification models was shown to severely reduce the overall reproducibility of the quantifications in our system. Our results emphasize that the gain of

accuracy associated with augmentation of quantification models must be validated against the corresponding loss of precision.

Quantification of mRNA by real-time RT-PCR consists of two experimental parts: the reverse transcription of RNA and the amplification and quantification of cDNA by PCR. Ståhlberg et al. [21] reported that in their system of absolute quantification the random error was larger in the reverse transcription step than in the PCR step. This problem is partly circumvented when performing relative quantification with reference genes, as in our setup. Nevertheless, random errors in the reverse transcription step, if differently affecting the transcription efficiency of the target genes and reference genes, would add to the errors discussed in this paper. The presented study focused on the effects of error propagation introduced by different quantification models in the PCR step only.

When comparing multiple quantifications of the same sample in separate experiments, we observed that the C_t values of different amplicons were correlated (Fig. 1 and Table 1). Thus, the covariance terms of the error propagation expressions could not be omitted. The correlation of C_t values between experimental runs was expected, since they depend heavily on the threshold fluorescence, which usually varies from run to run. Even though the fluorescence thresholds were set to a predefined value in all runs, we observed some correlation. This was probably due to the fact that the relationship between fluorescence and PCR product concentration varied from experiment to experiment. The same explanation lies behind the interassay variation of the constant k in Eq. (4) (Materials and methods) [5]. Furthermore, there is preliminary evidence that the C_t values of different transcripts quantitated in the same sample by multiplex PCRs are correlated even within the same experiment (unpublished observations). This indicates that at least in some multiplex assays covariances have to be included in both inter- and intraassay error propagation estimations.

Relative quantification of a specific mRNA can be defined as the amount of that mRNA relative to the amount of one or more reference mRNAs [4,7]. However, several groups use a different definition of relative quantification, defining the term as the amount of a specific mRNA in a sample relative to the amount of that mRNA in a control or calibrator sample [1,5]. The most common mathematical models for "relative" quantification include both levels of normalization, allowing both definitions to persist side by side. Calibrator normalization is expected to increase the accuracy and reproducibility of multirun experiments, allowing for better comparability between experiments. This is connected to the constant k in Eq. (4), which can vary from run to run [5]. In our system, however, calibrator normalization was shown to increase the overall random error of the quantification (Fig. 2). This indicated that the error caused by assuming that k is constant across the runs was smaller than the error increase caused by the calibrator. In our experimental system it thus seemed preferable to omit the calibrator normalization. However, in other experimental systems the calibrator may be more beneficial. In our experience, experimental changes such as new batches of primers can cause systematic changes in the C_t values measured for the same sample (unpublished observations). Likewise, Bustin et al. [3] has observed that different batches of TaqMan probes perform differently in quantification experiments. We suggest that the requirement for a calibrator should be validated in each experimental system. When calibrator normalization does not increase the overall interrun reproducibility of the quantification, we suggest using the calibrator to monitor the stability of the system rather than as a normalizer.

In the absence of perfect universal reference genes, Vandesompele et al. [24] proposed to normalize against the geometric mean of multiple reference genes. They argue that the geometric mean controls better for outlying values and abundance differences between the different reference genes. Averaging reference transcript concentrations is a challenging task, considering that the expression levels of different reference genes may vary over several orders of magnitude. The arithmetic mean would be more sensitive to changes in the levels of the most abundantly expressed reference genes than to changes in those with lower expression levels. Moreover, the arithmetic mean would give more complicated error propagation expressions. With the arithmetic mean in the denominator of Eq. (14) it is not possible to factorize out r_4 from the square root, as done in Eq. (15). Furthermore, the variance of the most abundant reference transcript will have greater impact on the overall error than that of the less abundant reference transcripts.

The analytical strength of real-time PCR lies in its wide dynamic range of quantitation, which may span up to seven orders of magnitude [22]. The reproducibility, however, may be less magnificent, especially at low concentrations. At very low concentrations ($C_t > 30$), there will be sampling error due to the stochastic movements of the few target molecules in the available volume (Poisson statistics) [21,22,32]. Furthermore, the exponential nature of PCR allows minor variations in reaction conditions and mispriming events in the early stages to be amplified throughout the process [2].

The amplification efficiency is usually lower than the maximal 2 and is not constant throughout the PCR. It has been suggested that the amplification efficiency is somewhat lower for the very first cycles due to the length of the original template and the first copies compared to the final PCR product [33]. Subsequently, the amplification efficiency stays reasonably constant until the depletion of reagents and accumulation of product inhibits the reaction, causing the efficiency to decrease toward zero. In addition, the amplification efficiencies of different amplicons are not necessarily identical but depend upon the length and sequence of the amplicons [34]. Thus, the use of specific amplification efficiencies for each amplicon seems highly adequate [7]. Moreover, evidence that the amplification efficiency

for each amplicon varies from sample to sample due to the presence of small amounts of PCR inhibitors from pre-PCR steps has been presented [15,17,29,30]. To correct for this apparent variation several strategies to determine amplification efficiencies from individual amplification curves have been proposed. The simplest approach is to perform linear regression on log-transformed data from the exponential part of the amplification curve [8,12–14]. The exponential part has been identified both manually and by various automatic or semiautomatic algorithms. Moreover, nonlinear regression of the exponential part of the amplification curve to an exponential function has been suggested [10,15,16]. Both these approaches focus exclusively on the exponential part of the amplification curve for the estimation of amplification efficiency. Contrary to this, others have proposed performing nonlinear regression of the entire amplification curve to a four-parametric sigmoidal model [9,11,17,18,31].

We tested three of the proposed strategies for determination of sample-specific amplification efficiencies, including the four-parametric sigmoidal-fit method of Liu and Saint, and obtained evidence that these determinations were imprecise (Figs. 4 and 5). The amplification efficiency variation of the same amplicon observed in different runs of the same sample seemed to reflect primarily random error of the determination and not a real variation. This is intriguing, considering the great interest that these ideas have engendered. However, our results are not entirely without support in the literature. Gentle et al. [8] used linear regression of the log-transformed exponential part of the amplification curve to determine sample-specific amplification efficiencies. However, they observed no significant difference in amplification efficiency in the samples and thus used a mean amplification efficiency in their quantifications. Peirson and co-workers [14] also used linear regression of log-transformed data from the exponential phase for amplification efficiency determination. They found no significant differences in amplification efficiency in different samples (ANOVA) and concluded that application of sample-specific amplification efficiencies appears unjustified. On the other hand, Tichopad and colleagues compared their exponential fit algorithm with the standard curve method (constant amplification efficiency for all quantifications of the same transcript) and the four-parametric-sigmoidal-fit algorithm of Liu and Saint. They showed that their algorithm was more precise than both the standard curve method and the Liu/Saint algorithm when computing an expression similar to Eq. (16) for a dilution series of the same sample. When we applied these methods on one of our standard curves, the standard curve method performed better than the other methods (CV% of 6.8%), contrary to Tichopad's results. We evaluated several standard curves and found that the performance in this kind of test depended upon the quality of the standard curve (results not shown). When there were substantial deviations from linearity, the standard curve method was less precise. This emphasizes the importance of validating that the real-time quantifications are in the linear range of the assay, at least when relying on the standard curve method for amplification efficiency determination. However, we cannot exclude that there might be instrument-dependent differences between the experiments, as Tichopad et al. performed their studies on a LightCycler (Roche) and we conducted ours on an Mx3000P instrument (Stratagene).

Bar and colleagues [15] determined sample-specific amplification efficiencies by fitting three to five points from the exponential part of the amplification curve to an exponential function. Optimizing the threshold defining the start of the exponential phase and the number of points used for regression, they achieved amplification efficiencies with rather low standard deviations when using purified PCR product as template. However, even if they applied their kinetic outlier detection algorithm to exclude samples with deviating amplification efficiencies they experienced considerable variation in relative quantifications of mRNA (mean CV% presented was 31%). In light of our results, it could even be questioned whether the kinetic outliers excluded were true outliers of the quantitation and not just the results of imprecise determination of amplification efficiency. It would have been interesting to compare the C_t values of their outliers with those of the nonoutliers.

Common to the linear and exponential fit-based methods are the dependence on rather few data points to determine the amplification efficiency. Often, only three to five points have been included in the regression analyses. Determination of two or three regression parameters from only three to five data points, fluorescence measurement noise taken into account, is in our opinion prone to be imprecise. It is not without reason that real-time data processing software often applies smoothing algorithms. Moreover, the data may not fit perfectly to the mathematical model applied for regression analysis, increasing the error of the parameter estimations. Bar et al. [15] report that their amplification efficiency determinations were sensitive to the selection of data points to be included in the regression analyses, confirming our reasoning. On the other hand, the signal/noise ratio of the fluorescence measurements may be different for other experimental setups. Thus, the random error of amplification efficiency determinations may vary for different instruments and detection chemistries.

The dependence on few data points is not a shortcoming of the four-parametric sigmoidal fit algorithm. Despite this, both our group and Tichopad et al. [17] experienced low precisions when using amplification efficiencies determined by this method in quantifications. However, the four-parametric sigmoidal model also allows quantification by computation of the initial fluorescence after background subtraction. Rutledge [18] presents evidence that this quantification strategy produces data with high reproducibility. In our hands, using cDNA as template, this strategy (implemented as in [9]) was very sensitive to the background subtraction and produced less precise quantifications (results not shown). Moreover, the conversion from initial fluorescence to template concentration is not straightforward and

depends upon the relationship between fluorescence and PCR product amount. It is also unclear to us how the background phase of amplification curves can contain information about the initial amount of template, especially when using randomly primed cDNA as template.

With respect to the presented evidence on imprecise determination of amplification efficiencies from individual amplification curves, we suggest that the standard curve method should still be used for determination of amplification efficiencies. However, the standard curve method also suffers from random error. Thus, amplicon-specific efficiencies should be determined from multiple standard curves with several replicates of each dilution to minimize the random error of the determination.

Although becoming a standard technique for mRNA quantification, the data processing framework of real-time RT-PCR is still in development. We emphasize the importance of validating new mathematical quantification models in view of error propagation. Increasing the complexity of the models also has the potential to reduce reproducibility, as we have shown herein. Gain of accuracy associated with the development of new models must be balanced against the possible loss of precision.

Acknowledgments

This work was supported by the Norwegian Cancer Society and the Western Norway Regional Health Authority.

Appendix A. Supplementary data

Supplementary data associated with this article can be found, in the online version, at doi:10.1016/j.ab.2006.06.020.

References

[1] M.L. Wong, J.F. Medrano, Real-time PCR for mRNA quantitation, Biotechniques 39 (2005) 75–85.
[2] S.A. Bustin, Absolute quantification of mRNA using real-time reverse transcription polymerase chain reaction assays, J. Mol. Endocrinol. 25 (2000) 169–193.
[3] S.A. Bustin, Quantification of mRNA using real-time reverse transcription PCR (RT-PCR): trends and problems, J. Mol. Endocrinol. 29 (2002) 23–39.
[4] K. Edwards, J. Logan, N. Saunders (Eds.), Real-Time PCR: An Essential Guide, Horizon Bioscience, London, 2004.
[5] K.J. Livak, T.D. Schmittgen, Analysis of relative gene expression data using real-time quantitative PCR and the 2(-Delta Delta C(T)) Method, Methods 25 (2001) 402–408.
[6] R. Rasmussen, in: S. Meuer, C. Wittwer, K. Nakagawaras (Eds.), Rapid Cycle Real-time PCR, Methods and Applications, Springer Press, 2001, pp. 21–34.
[7] M.W. Pfaffl, A new mathematical model for relative quantification in real-time RT-PCR, Nucleic Acids Res. 29 (2001) e45.
[8] A. Gentle, F. Anastasopoulos, N.A. McBrien, High-resolution semi-quantitative real-time PCR without the use of a standard curve, Biotechniques 31 (2001) 502, 504–506, 508.
[9] W. Liu, D.A. Saint, Validation of a quantitative method for real time PCR kinetics, Biochem. Biophys. Res. Commun. 294 (2002) 347–353.
[10] W. Liu, D.A. Saint, A new quantitative method of real time reverse transcription polymerase chain reaction assay based on simulation of polymerase chain reaction kinetics, Anal. Biochem. 302 (2002) 52–59.
[11] A. Tichopad, A. Dzidic, M. Pfaffi, Improving quantitative real-time RT-PCR reproducibility by boosting primer-linked amplification efficiency, Biotechnol. Lett. 24 (2002) 2053–2056.
[12] C. Ramakers, J.M. Ruijter, R.H. Deprez, A.F. Moorman, Assumption-free analysis of quantitative real-time polymerase chain reaction (PCR) data, Neurosci. Lett. 339 (2003) 62–66.
[13] J.H. Marino, P. Cook, K.S. Miller, Accurate and statistically verified quantification of relative mRNA abundances using SYBR Green I and real-time RT-PCR, J. Immunol. Methods 283 (2003) 291–306.
[14] S.N. Peirson, J.N. Butler, R.G. Foster, Experimental validation of novel and conventional approaches to quantitative real-time PCR data analysis, Nucleic Acids Res. 31 (2003) e73.
[15] T. Bar, A. Ståhlberg, A. Muszta, M. Kubista, Kinetic outlier detection (KOD) in real-time PCR, Nucleic Acids Res. 31 (2003) e105.
[16] A. Tichopad, M. Dilger, G. Schwarz, M.W. Pfaffl, Standardized determination of real-time PCR efficiency from a single reaction set-up, Nucleic Acids Res. 31 (2003) e122.
[17] A. Tichopad, A. Didier, M.W. Pfaffl, Inhibition of real-time RT-PCR quantification due to tissue-specific contaminants, Mol. Cell. Probes 18 (2004) 45–50.
[18] R.G. Rutledge, Sigmoidal curve-fitting redefines quantitative real-time PCR with the prospective of developing automated high-throughput applications, Nucleic Acids Res. 32 (2004) e178.
[19] D.A. Skoog, D.M. West, H.F. J, Fundamentals of analytical chemistry, Saunders College publishing, Orlando, 1991.
[20] A.A. Clifford, Multivariate Error Analysis: A Handbook of Error Propagation and Calculation in Many-Parameter System, Applied Science Publishers Ltd, London, 1973.
[21] A. Ståhlberg, J. Hakansson, X. Xian, H. Semb, M. Kubista, Properties of the reverse transcription reaction in mRNA quantification, Clin. Chem. 50 (2004) 509–515.
[22] T.B. Morrison, J.J. Weis, C.T. Wittwer, Quantification of low-copy transcripts by continuous SYBR Green I monitoring during amplification, Biotechniques 24 (1998) 954–958, 960, 962.
[23] O. Thellin, W. Zorzi, B. Lakaye, B. De Borman, B. Coumans, G. Hennen, T. Grisar, A. Igout, E. Heinen, Housekeeping genes as internal standards: use and limits, J. Biotechnol. 75 (1999) 291–295.
[24] J. Vandesompele, K. De Preter, F. Pattyn, B. Poppe, N. Van Roy, A. De Paepe, F. Speleman, Accurate normalization of real-time quantitative RT-PCR data by geometric averaging of multiple internal control genes, Genome Biol. 3 (2002), RESEARCH0034.
[25] K. Dheda, J.F. Huggett, S.A. Bustin, M.A. Johnson, G. Rook, A. Zumla, Validation of housekeeping genes for normalizing RNA expression in real-time PCR, Biotechniques 37 (2004) 112–114, 116, 118–119.
[26] J.L. Aerts, M.I. Gonzales, S.L. Topalian, Selection of appropriate control genes to assess expression of tumor antigens using real-time RT-PCR, Biotechniques 36 (2004) 84–86, 88, 90–91.
[27] C.L. Andersen, J.L. Jensen, T.F. Orntoft, Normalization of real-time quantitative reverse transcription-PCR data: a model-based variance estimation approach to identify genes suited for normalization, applied to bladder and colon cancer data, Cancer Res. 64 (2004) 5245–5250.
[28] J.B. de Kok, R.W. Roelofs, B.A. Giesendorf, J.L. Pennings, E.T. Waas, T. Feuth, D.W. Swinkels, P.N. Span, Normalization of gene expression measurements in tumor tissues: comparison of 13 endogenous control genes, Lab. Invest. 85 (2005) 154–159.
[29] L. Rossen, P. Norskov, K. Holmstrom, O.F. Rasmussen, Inhibition of PCR by components of food samples, microbial diagnostic assays and DNA-extraction solutions, Int. J. Food Microbiol. 17 (1992) 37–45.
[30] I.G. Wilson, Inhibition and facilitation of nucleic acid amplification, Appl. Environ. Microbiol. 63 (1997) 3741–3751.
[31] M.P. Johnson, L.M. Haupt, L.R. Griffiths, Locked nucleic acid (LNA) single nucleotide polymorphism (SNP) genotype analysis and validation using real-time PCR, Nucleic Acids Res. 32 (2004) e55.

[32] J. Stenman, A. Orpana, Accuracy in amplification, Nat. Biotechnol. 19 (2001) 1011–1012.
[33] H.K. Nogva, K. Rudi, Potential influence of the first PCR cycles in real-time comparative gene quantifications, Biotechniques 37 (2004) 246–248, 250–253.
[34] J. Chelly, D. Montarras, C. Pinset, Y. Berwald-Netter, J.C. Kaplan, A. Kahn, Quantitative estimation of minor mRNAs by cDNA-polymerase chain reaction. Application to dystrophin mRNA in cultured myogenic and brain cells, Eur. J. Biochem. 187 (1990) 691–698.